ACCOUNTS of chemical research

Article

pubs.acs.org/accounts

Optically Modulated Fluorescence Bioimaging: Visualizing Obscured Fluorophores in High Background

Jung-Cheng Hsiang,[†,§] Amy E. Jablonski,[‡,§] and Robert M. Dickson*[,‡,§]

[†]School of Physics, [‡]School of Chemistry & Biochemistry, and [§]Petit Institute of Bioscience and Bioengineering, Georgia Institute of Technology, Atlanta, Georgia 30332-0400, United States

CONSPECTUS: Fluorescence microscopy and detection have become indispensible for understanding organization and dynamics in biological systems. Novel fluorophores with improved brightness, photostability, and biocompatibility continue to fuel further advances but often rely on having minimal background. The visualization of interactions in very high biological background, especially for proteins or bound complexes at very low copy numbers, remains a primary challenge. Instead of focusing on molecular brightness of fluorophores, we have adapted the principles of high-sensitivity absorption spectroscopy to improve the sensitivity and signal discrimination in fluorescence bioimaging.

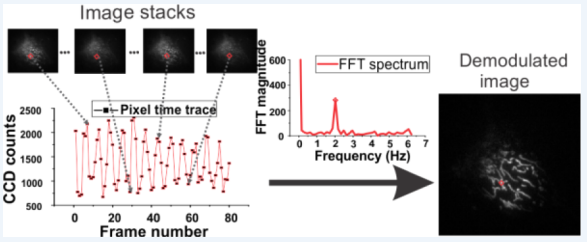

Utilizing very long wavelength transient absorptions of kinetically trapped dark states, we employ molecular modulation schemes that do not simultaneously modulate the background fluorescence. This improves the sensitivity and ease of implementation over high-energy photoswitch-based recovery schemes, as no internal dye reference or nanoparticle-based fluorophores are needed to separate the desired signals from background.

In this Account, we describe the selection process for and identification of fluorophores that enable optically modulated fluorescence to decrease obscuring background. Differing from thermally stable photoswitches using higher-energy secondary lasers, coillumination at very low energies depopulates transient dark states, dynamically altering the fluorescence and giving characteristic modulation time scales for each modulatable emitter. This process is termed synchronously amplified fluorescence image recovery (SAFIRe) microscopy. By understanding and optically controlling the dye photophysics, we selectively modulate desired fluorophore signals independent of all autofluorescent background. This shifts the fluorescence of interest to unique detection frequencies with nearly shot-noise-limited detection, as no background signals are collected.

Although the fluorescence brightness is improved slightly, SAFIRe yields up to 100-fold improved signal visibility by essentially removing obscuring, unmodulated background (Richards, C. I.; et al. *J. Am. Chem. Soc.* **2009**, *131*, 4619). While SAFIRe exhibits a wide, linear dynamic range, we have demonstrated single-molecule signal recovery buried within 200 nM obscuring dye. In addition to enabling signal recovery through background reduction, each dye exhibits a characteristic modulation frequency indicative of its photophysical dynamics. Thus, these characteristic time scales offer opportunities not only to expand the dimensionality of fluorescence imaging by using dark-state lifetimes but also to distinguish the dynamics of subpopulations on the basis of photophysical versus diffusional time scales, even within modulatable populations. The continued development of modulation for signal recovery and observation of biological dynamics holds great promise for studying a range of transient biological phenomena in natural environments. Through the development of a wide range of fluorescent proteins, organic dyes, and inorganic emitters that exhibit significant dark-state populations under steady-state illumination, we can drastically expand the applicability of fluorescence imaging to probe lower-abundance complexes and their dynamics.

1. INTRODUCTION

Spectroscopy has proven to be crucial for understanding the structures and kinetics of myriad molecules and their environmental interactions. For example, analysis of the fingerprint region using infrared spectroscopy routinely enables resolution of multiple components constituting complex, unknown samples.[1] Unfortunately, such molecule-specific spectroscopic signatures are obscured in condensed phase, ambient temperature electronic spectroscopies. This fact limits the identification of molecular signatures in high-background samples and often relegates both single-molecule and bulk spectroscopies to rigorous exclusion of unwanted absorbers to minimize interference. However, even with ideal sample preparation, no measurement is truly "background-free". In absorption experiments, one must detect the change in incident laser intensity resulting from (typically weak) sample absorption. Thus, fluctuations in laser intensity become a primary noise source.[2] In pure systems, one can circumvent laser, detector, and other spurious noise sources by modulating the signal of interest and detecting at this modulation frequency, shifted away from the majority of laser noise. Such studies are also routinely performed to enhance the sensitivities of sequential and simultaneous multiphoton spectroscopies.[3] The key aspect is to encode an external waveform exclusively on the signal of interest, enabling its detection without interference from other species. Typically,

Received: January 25, 2014
Published: April 14, 2014

   dx.doi.org/10.1021/ar400325y | *Acc. Chem. Res.* 2014, 47, 1545−1554

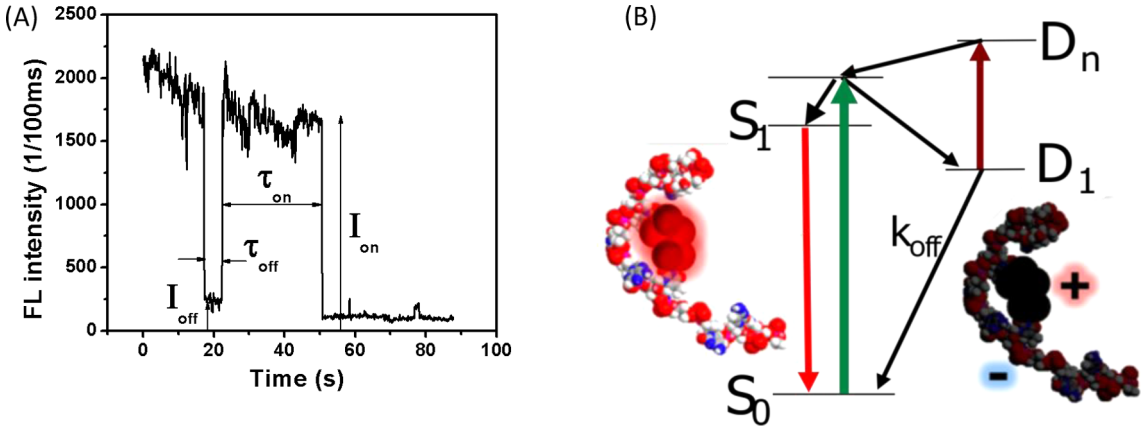

Figure 1. (A) Typical fluorescence blinking from a single silver nanodot (900 nm emitter). (B) Jablonski diagram illustrating the reverse intersystem crossing between bright and dark states of silver−DNA nanodots. (Reproduced with permission from ref 20. Copyright 2013 American Chemical Society.)

molecular modulation is the most sensitive, allowing the detection of changes in incident laser intensity ($\Delta I/I$) of $\sim 10^{-6}$ that result from molecular absorption.[2]

When molecules with high fluorescence quantum yields are used, fluorescence detection offers further gains in detection sensitivity, as the excitation light is filtered out to recover "zero-background" signals at a wavelength that is shifted to lower energy than that of the excitation source. For pure samples, the sensitivity is primarily limited by shot noise from the fluorophore and background instead of that from the much brighter excitation source. In complex systems, however, multiple fluorophores are often present that obscure signals from the desired emitters. This is especially true in biological samples and can preclude the observation of species of interest in natural environments, too often relegating mechanistic studies to artificial in vitro conditions. Even studies of bulk photophysical dynamics can be obscured by high background or low dark-state quantum yields, such that observation is facilitated by recording fluctuations at very low copy numbers.[4,5]

While researchers have made great advances by improving the brightness, spectral coverage, and biocompatibility of fluorescent probes,[6,7] these only address the signal side of sensitivity (signal-to-noise ratio). We have endeavored to make even greater sensitivity gains by decreasing the noise and simultaneously increasing only our desired signal visibility in high-background environments.[8−10] To accomplish this, we have applied the principles of modulated spectroscopy to fluorescence imaging. By investigating and tailoring dye photophysics, we have created systems whose fluorescence can be dynamically increased and decreased (modulated) through coillumination at much lower energy than that of the collected fluorescence.[11−15] Thus, we utilize the spectroscopy of transient dark states that normally limit fluorescence emission but themselves can be directly depopulated faster than they normally decay to alter fluorophore ground-state populations.

Generally, organic dyes offer excellent brightness with broad spectral tunability and small size; quantum dots exhibit further-improved brightness and photostability, but at the cost of toxicity, size, and aggregation, while fluorescent proteins greatly increase the biocompatibility, but at the cost of total brightness. While these different fluorophores can be useful in many conventional applications, exogenous or endogenous background fluorescence, especially in low-copy-number or multiple-labeling schemes, can seriously limit direct interpretation.[4] In such situations, the key issue becomes signal discrimination to enable resolution of each unique fluorophore's signal independent of the background. Time gating using very long lived (often lanthanide-based) fluorophores with pulsed excitation is one approach, as background emitters typically finish fluorescing within 10 ns of the pulsed excitation, reducing the background at longer delays.[16] Frequency domain approaches (e.g., optical lock-in detection[17] and frequency domain imaging[18]) use repetitive photobleaching of slowly responsive photoswitches with bursts of higher-energy secondary laser irradiation for fluorescence recovery. Because both lasers are at higher energy than the collected emission, an internal reference signal must be added or multidye nanoparticles must be used. The signal from the brighter nanoparticles is recovered mixed with the modulated background, or when more standard dye labeling is used, signals are better discriminated from the modulated background through cross-correlation with known pure-dye reference signals. Our efforts have been focused on a more direct analogy between modulation and fluorescence to selectively encode a modulation waveform only on the fluorophores of interest without also modulating the background. This process of synchronously amplified fluorescence image recovery (SAFIRe)[14] is also a frequency domain technique used to recover the signal of interest from the background. Importantly, as the background is not modulated and molecule-specific absorptions at lower energy than collected emission are utilized to modulate transient dark-state and ground-state populations, SAFIRe modulates fluorescence signals faster without introducing extra background emission, can be used to extract a large demodulation signal without the need to introduce a pure-dye external reference, and can provide molecule-specific dark-state lifetimes to expand the dimensionality of fluorescence imaging.[11] In this Account, we will describe the principles behind SAFIRe, its attainable contrast improvement, fluorophore development, dye photophysical properties, and recent applications of SAFIRe for signal recovery in bioimaging.

2. FLUORESCENCE ENHANCEMENT THROUGH DARK-STATE DEPOPULATION

For fluorescent molecules, the singlet−singlet radiative emission is often hindered by residence in long-lived triplet states, exciton traps, photoisomers, charge-transfer states, or other dark states. Once the molecule reaches the dark state, it generally takes some finite time for the molecule to relax back to its emissive state,

dx.doi.org/10.1021/ar400325y | Acc. Chem. Res. 2014, 47, 1545−1554

Table 1. Photophysical Parameters of Ag Nanoclusters[23]

species	ssDNA sequence	emission wavelength (nm)	lifetime (ns)	Φ (%)	ε (10^5 M^{-1} cm^{-1})
blue	5′-CCCTTTAACCCC-3′	485	2.98 ± 0.01	NA	NA
green	5′-CCCTCTTAACCC-3′	520	0.22 ± 0.01	16 ± 3	NA
yellow	5′-CCCTTAATCCCC-3′	572	4.35 ± 0.01	38 ± 2	2.0 ± 0.4
red	5′-CCTCCTTCCTCC-3′	620	2.23 ± 0.01	32 ± 4	1.2 ± 0.3
near-IR	5′-CCCTAACTCCCC-3′	705	3.46 ±.01	34 ± 5	3.5 ± 0.7

leading to a steady-state buildup of this nonemissive level. This stochastic on and off "blinking" (Figure 1A) has a steady-state fluorescence intensity of

$$I_{avg} = \frac{\tau_{on}}{\tau_{on} + \tau_{off}^0} I_{on} + \frac{\tau_{off}^0}{\tau_{on} + \tau_{off}^0} I_{off}$$

in which τ_{on} and τ_{off}^0 are the intrinsic photophysical on and off times, characterizing how long the molecule stays in the emissive and dark-state manifolds, respectively, I_{on} is the on-time fluorescence intensity, and I_{off} is the off-time intensity (usually zero). This population recovery from the dark states of some common fluorophores can be effected with exceedingly high intensity (MW/cm^2), application-limiting, red-shifted secondary excitation.[19] Such long-wavelength coillumination presumably induces an inefficient reverse intersystem crossing (ISC) process that alters (reduces) the steady-state dark-state population to increase the fluorescence emission rate (Figure 1B). Our goal has been to drastically reduce the necessary secondary intensities by probing the transient absorptions of these long-lived photoaccessible dark states. Such sequential two-photon excitation increases the fluorescence intensities with reasonably low secondary laser intensities (1−100 kW/cm^2) by decreasing the steady-state dark-state residence to enable more fluorophores to absorb and fluoresce under primary excitation. The relative enhancement factor is defined as

$$\text{relative enhancement factor} = \frac{I_{dual} - I_{primary}}{I_{primary}} = \frac{\tau_{off}^0 - \tau_{off}}{\tau_{on} + \tau_{off}}$$

in which $I_{primary}$ and I_{dual} are the fluorescence intensities with primary-only and dual laser excitation, respectively, and τ_{off} is the photophysical off time with dual laser excitation.[14] Thus, to achieve high enhancement, the fluorophores should exhibit relative on and off times subject to (1) $\tau_{on} < \tau_{off}^0$ and (2) $\tau_{off} \ll \tau_{off}^0$. These conditions generally hold for dyes exhibiting the following properties:[14]

(1) A naturally decaying dark state exhibiting some characteristic decay time.
(2) Dark-state absorption at lower energy than that of the collected fluorescence.
(3) High forward action cross sections (extinction coefficient times dark-state quantum yield), enabling low primary illumination intensities.
(4) High reverse action cross sections for dark-state depopulation, enabling low secondary illumination intensities.

When the above conditions are met, the maximum relative enhancement factor is determined by τ_{off}^0/τ_{on}, corresponding to complete removal of the dark-state residence through secondary laser coillumination (i.e., τ_{off} goes to zero).

3. OPTICALLY ENHANCEABLE FLUOROPHORES

The crucial requirement for optically enhanced fluorescence is to have a relatively long lived but long-wavelength optically reversible dark state. Thus, microsecond to millisecond transient absorption spectroscopy and fluorescence correlation spectroscopy (FCS) studies are exceedingly helpful in identifying candidate fluorophores and guiding secondary laser selection.[5,8,14] In principle, any transient photoinduced dark state can suffice (e.g., triplet, photoisomer, charge separation, etc.) as long as it decays on its own and its natural lifetime is comparable to or longer than the inverse excitation rate. Below we discuss the most promising enhanceable fluorophores that we have identified to date.

3.1. Silver Nanodots

Few-atom silver nanodots (less than ∼12 Ag atoms) become stable in solution only with the help of protective scaffolds.[20,21] However, the choice of scaffold not only determines which nanodot species is formed but also is crucial for optical enhancement of its fluorescence. Through the use of these different scaffolds, many single-stranded DNA (ssDNA)-protected silver nanodots have been successfully synthesized and photophysically characterized, yielding strong emitters extending from the visible to the near-IR.[22,23] Table 1 lists a small subset of our emitters and their basic photophysical parameters.

The strong nucleobase−Ag interaction and suggestive transient absorption/FCS studies[5,24] coupled with the known propensity of Ag nanoclusters to photoeject electrons[25] led us to the conclusion that a ∼10 μs-lived charge-separated dark state is the likely modulatable level. Common among all of the DNA-encapsulated Ag nanodots studied, the transient absorption spectra suggested that the common red absorption band (650−850 nm) arises from anionic cytosine absorption that decays via reverse charge transfer. Nicely matching the fluorescence enhancement action spectrum, this provides a framework for rationalizing how the dark-state lifetime decreases and the total (higher-energy) fluorescence intensity increases upon coillumination at 800 nm.[8]

3.2. Organic Fluorophores

Myriad fluorescent organic compounds have been employed in fluorescence spectroscopy and microscopy because of their synthetic tunability, bright emission, and wide availability. The excited-state photophysics of many common fluorophores have been mapped out through transient absorption and FCS studies, and some have even been demonstrated to undergo reverse ISC under very high intensity (>1 MW/cm^2) dual laser excitation.[19,26] Some weak emitters, however, build up large dark-state populations with strong transient absorptions that are significantly red-shifted from their fluorescent transitions. Cy5, for example, exhibits forward and reverse ISC from short-lived triplet levels and rapidly photoisomerizes between the trans ground state and the relatively long lived, red-shifted cis dark state.[27,28] In agreement with the transient absorption studies,[27] a

dx.doi.org/10.1021/ar400325y | Acc. Chem. Res. 2014, 47, 1545−1554

near-IR secondary laser efficiently optically reverses the photoisomerization, thereby modulating the *trans*-Cy5 emission. Many fluorophores, including various cyanines and multiple fluorescein and rhodamine derivatives, exhibit fluorescence that can be optically enhanced for signal improvement through long-wavelength coillumination.[19,29] The nature of these transient but photoreversible dark states varies from triplets to photoisomers, but all are useful because of their ability to dynamically increase the fluorescence through optical depletion of the long-lived dark states.[11,28]

3.3. Fluorescence Resonance Energy Transfer (FRET) Pairs

Multiple FRET techniques have been proposed to circumvent the drawbacks of many natural fluorescent organic compounds.[30] Frustrated FRET,[31,32] in which a red secondary laser is used to saturate the acceptor in order to manipulate the higher-energy donor fluorescence, is ideal for conferring modulatability only on bound complexes. Similar to the use of stimulated emission depletion (STED) to frustrate fluorescence,[12] coupling unmodulatable molecules together and optically frustrating their FRET creates modulatable composite dyes. Specifically, we attached fluorescein and tetramethylrhodamine (TMR) to opposite ends of hairpin DNA (Figure 2). Because of energy transfer, TMR quenched the fluorescein emission. We demonstrated that we could dynamically increase the donor emission by optically frustrating FRET through direct acceptor saturation, even though neither dye is individually enhanceable on its own.[15] By utilizing acceptors with longer dark-state lifetimes, we further improved the donor fluorescence enhancement at lower excitation intensities. In principle, this can be done to create optically enhanceable donors only when species are bound, thereby potentially enabling the measurement of binding constants in high-background environments.

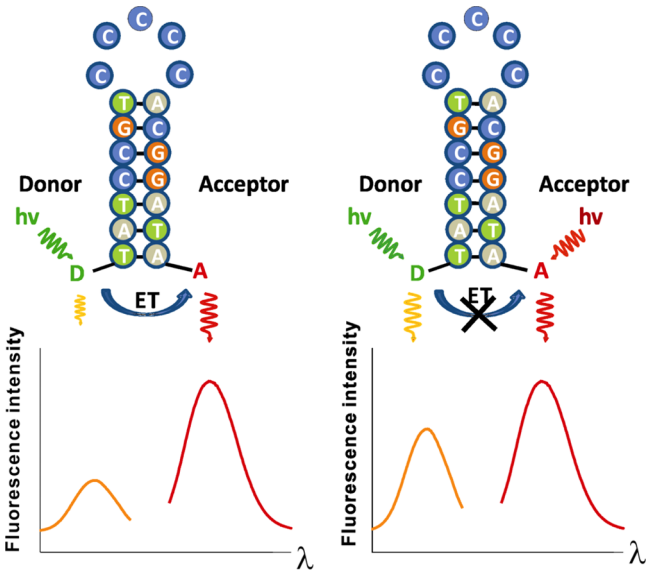

Figure 2. Schematic of SAFIRe using FRET pairs on hairpin-forming ssDNA. (A) Typical energy transfer from donor to acceptor with donor excitation only. (B) Saturation of the acceptor excitation can block (or modulate) energy transfer, thereby increasing donor emission through frustrated FRET. (Reproduced with permission from ref 15. Copyright 2010 American Chemical Society.)

3.4. Fluorescent Proteins

The discovery of fluorescent proteins has revolutionized cell biology, as both in vivo and in vitro dynamics and statics can be readily studied with one-to-one labeling, genetic encodability, and excellent biocompatibility.[7] While much effort has gone into creating fluorescent protein derivatives with improved brightness, photostability, and spectral coverage, many recent efforts have focused on their photoswitching properties.[33] Since the first discoveries of the photoswitching properties of green fluorescent protein derivatives (GFPs),[34,35] studies of multiple derivatives[36,37] have demonstrated that different wavelengths of light can induce forward and reverse photoisomerization. The fluorophore's propensity to undergo excited-state proton transfer offers the unique ability to tune the chromophore environment, further changing the isomerization barriers and protonation-state thermodynamics.[38] Because of these photoreversible states, we postulated that the photoisomers should also have long-wavelength absorptions that could optically regenerate the emissive state. To date, we have identified blue fluorescent proteins (BFPs) and GFPs capable of optically enhanced fluorescence.[9,13] Furthermore, by altering the amino acids surrounding the fluorophore, we have demonstrated that we can both shift the dark-state absorption to longer wavelengths and improve the magnitude of the fluorescence enhancement upon secondary illumination (Table 2).[9,13]

4. DYNAMICALLY ALTERING GROUND-STATE POPULATIONS: FLUORESCENCE MODULATION

Upon primary excitation, all modulatable dyes exhibit an initial burst of bulk fluorescence with a decrease to the steady-state intensity as the dark-state population builds. Secondary coillumination at wavelengths longer than those of the collected fluorescence restores the higher ground-state population, increasing the steady-state fluorescence with both lasers illuminating the sample while generating no additional background. Turning the secondary laser on and off switches between brighter and dimmer steady-state fluorescence intensities. If the secondary laser intensity is modulated at a specific frequency, the fluorescence intensity will also be modulated at the exact same frequency.[8] Thus, through dynamic control of the ground-state population with very long wavelength secondary coexcitation,

Table 2. Summary of the Compounds Used in SAFIRe

fluorophore	primary/secondary excitation wavelength (nm)	typical relative enhancement (%)	typical cutoff frequency (Hz)	ref(s)
silver clusters	varies/800	100	100k	5, 8
Cy5	594/710	40	30k	11
rose bengal	532/910	100	333k	14
engineered FRET pairs	varies/varies	varies	varies	15
modBFP	372/514	20	16	13
modBFP/H148K	372/514	37	37	13
AcGFP	476/561	8	800	9

dx.doi.org/10.1021/ar400325y | *Acc. Chem. Res.* 2014, 47, 1545−1554

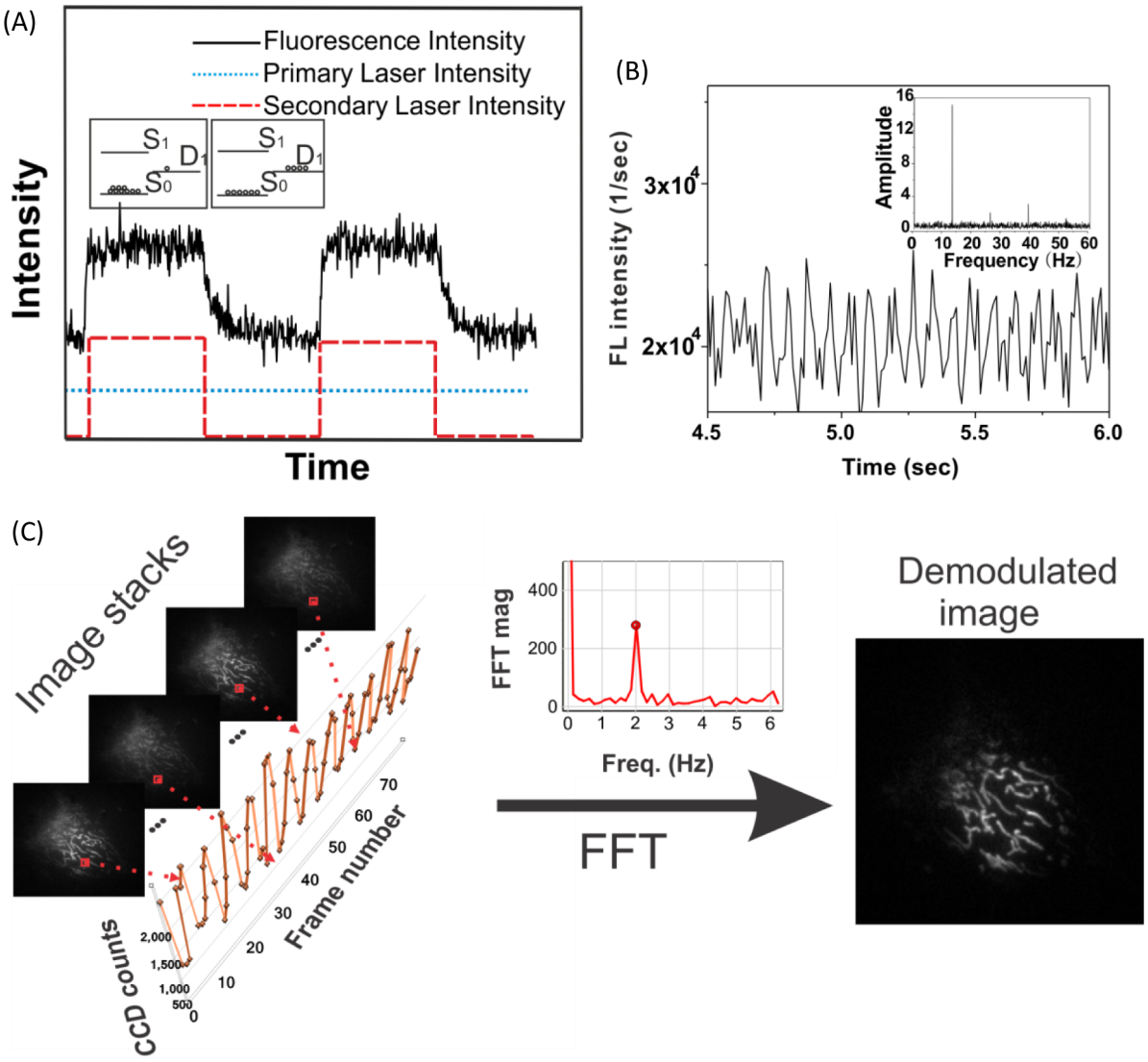

Figure 3. (A) Fluorescence response of an optically modulatable blue fluorescent protein (modBFP/H148K) with constant primary excitation and modulated secondary excitation. The insets show Jablonski diagrams representing dark/bright populations. (B) Time trace of aqueous modBFP/H148K with 372 nm primary excitation and 514 nm secondary excitation modulated at 13 Hz. The inset shows the fast Fourier transform (FFT) of the bulk intensity trajectory, recovering the modulation frequency encoded in the fluorescence signal. (C) Analysis of optically modulated image stacks acquired with SAFIRe by taking the Fourier transform of each pixel's intensity trajectory. The demodulated image is formed from the FFT amplitude at each pixel.

the fluorescence of interest is shifted away from all of the background to a unique detection frequency without either generating any additional background that can obscure detection or increasing the photobleaching quantum yields.[9] As demonstrated below, this directly enables the extraction of molecular signatures within complex environments and avoids signals from competing fluorophores—some by increasing the signal but mostly by decreasing the background within the detection window. Such an optical fluorescence modulation and demodulation process is what we have termed synchronously amplified fluorescence image recovery (SAFIRe) microscopy.

5. SENSITIVITY IMPROVEMENT: SAFIRE

Amplitude modulation techniques have been widely used in high-fidelity signal transmission and recovery, as desired or encoded signals are shifted to specific frequencies exhibiting greatly reduced background. If fluorophore signals can be selectively modulated, their signals will shift away from the unmodulated background, drastically improving their visibility and signal-to-noise ratio (SNR). In photon counting experiments, the unmodulated fluorescence intensity, $i_1(t)$, is

$$i_1(t) = n_S(t) + n_B(t)$$

in which $n_S(t)$ is the number of signal photons at steady state and $n_B(t)$ is the number of uniform background counts. Steady-state dark-state populations can be altered through secondary coillumination, and amplitude modulation of this secondary laser yields a fluorescence intensity $i_2(t)$ given by

$$i_2(t) = n_S(t) + \frac{mn_S(t)}{2}[1 + \cos(1 + 2\pi ft)] + n_B(t)$$

in which m is the relative fluorescence enhancement factor and f is the sinusoidal modulation frequency. In shot-noise-limited photon counting measurements, the SNRs without and with modulation, respectively, are

dx.doi.org/10.1021/ar400325y | Acc. Chem. Res. 2014, 47, 1545−1554

$$\mathrm{SNR}_1 = \frac{n_S\sqrt{N}}{\sqrt{n_S + n_B}} \quad (1)$$

and

$$\mathrm{SNR}_2 = \frac{mn_S\sqrt{N}}{\sqrt{n_S + mn_S + n_B}} \quad (2)$$

in which N is the number of bins in the measurement. Equations 1 and 2 demonstrate that when there exists uniform, high exogenous fluorescence contamination or when the fluorescence intensity is relatively low compared with the background, there is little SNR advantage unless the relative enhancement factor is much larger than 1.

The true practical challenge is one of signal visibility. When a weak signal is buried within a high or spatially heterogeneous background, one is often unable to separate signal photons from background photons, rendering weak signals invisible. In bioimaging applications, the commonly observed heterogeneous background around regions of interest precludes discerning between the desired signal and unwanted background a priori. Thus, the more important metric is signal visibility, or the signal-to-background ratio (SBR), to quantify the imaging quality/contrast of the fluorophore of interest. Different from eqs 1 and 2, the SBRs without and with modulation/demodulation, respectively, are

$$\mathrm{SBR}_1 = \frac{n_S}{n_B} \quad (3)$$

$$\mathrm{SBR}_2 = \frac{mn_S\sqrt{N}}{\sqrt{n_B}} \quad (4)$$

From eqs 3 and 4, one sees that SAFIRe efficiently increases the SBR and thus the image contrast, even with high heterogeneous background levels. This major advantage makes visible features that are otherwise obscured, enabling their quantification by recovery of shot-noise-limited detection sensitivities through shifting the signal to specific narrow-band detection (modulation) frequencies that are free from background interference (Figure 3).

6. SWITCHING SPEED

In SAFIRe, the enhancement results from repumping molecules from the dark state to the emissive manifold faster than through natural dark-state decay. Thus, the rates into and out of the dark state define the characteristic frequency (or inverse characteristic time) for establishing these steady-state populations. Consequently, compounds should exhibit characteristic cutoff frequencies in their modulation frequency response curves.

At low excitation intensities, a singlet−singlet transition with a natural excited-state lifetime τ_0 yields a normalized frequency response $R(f)$ given by[39]

$$R(f) = \frac{1}{\sqrt{(2\pi f)^2 + \tau_0^{-2}}}$$

Similarly, fluorescent molecules with one photophysical on time τ_{on} and one off time τ_{off} have an intrinsic optical response time τ_c given by

$$\tau_c = (\tau_{on}^{-1} + \tau_{off}^{-1})^{-1} = (I_{ex}\sigma\phi_{ISC} + \tau_{dark}^{-1})^{-1} \quad (5)$$

in which I_{ex} is the excitation intensity, σ is the absorption cross section, ϕ_{ISC} is the ISC quantum yield, and τ_{dark} is the intrinsic dark-state relaxation time. Whenever the external driving frequency is much higher than the inverse characteristic response time τ_c^{-1}, the molecules cannot fully respond, decreasing the fluorescence enhancement or modulation depth at these high frequencies. Hence, analogous to a frequency-domain lifetime measurement, scanning the scaled modulation frequency generates a modulation depth versus frequency response curve for a bulk sample that is given by

$$m(f) = \frac{1}{\sqrt{(2\pi f)^2 + \tau_c^{-2}}} \quad (6)$$

Fitting response curves to this model yields the intrinsic response time τ_c, which represents the time necessary to establish steady-state ground- and dark-state populations, or the frequency at which the modulation depth decreases by 50%. An example of this, Figure 4 shows characteristic frequency response curves of

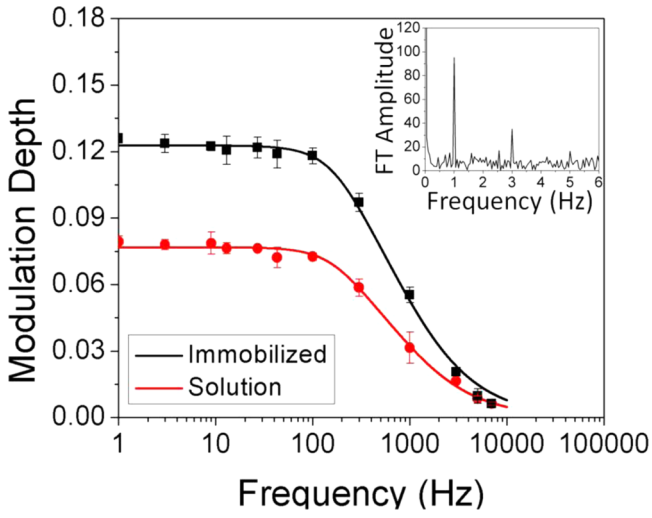

Figure 4. Modulation frequency dependence of AcGFP enhancement at 561 nm for immobilized (red) and diffusing (black) molecules. The modulation depth at each frequency was computed by normalizing the doubled Fourier transform of each time trace by the number of data points and by its DC component. The inset shows the Fourier transform of the square-wave-modulated fluorescence of AcGFP at 1 Hz. (Reproduced with permission from ref 9. Copyright 2012 American Chemical Society.)

AcGFP and the corresponding fitted curves.[9] This opens the potential for discriminating otherwise identical fluorophores on the basis of their dark-state or characteristic lifetimes (Figure 5A). Furthermore, eqs 5 and 6 suggest that one can also manipulate the characteristic cutoff frequency simply by changing the excitation intensity, as demonstrated in Figure 5B. Consequently, one has the option of tuning the characteristic frequency to match the dynamics under study. Any change in the characteristic frequency could then be interpreted as a change in molecular dynamics (e.g., diffusion, binding, etc.) that effectively depopulates the dark level, replacing it with a fluorophore in its emissive manifold.

7. APPLICATIONS

Three crucial aspects of SAFIRe distinguish it from photoswitch-based methods: (1) Because modulated low-energy (lower than that of collected fluorescence) secondary illumination is used, SAFIRe modulates only the desired signal—it does not modulate the background. (2) The externally defined secondary laser

dx.doi.org/10.1021/ar400325y | Acc. Chem. Res. 2014, 47, 1545−1554

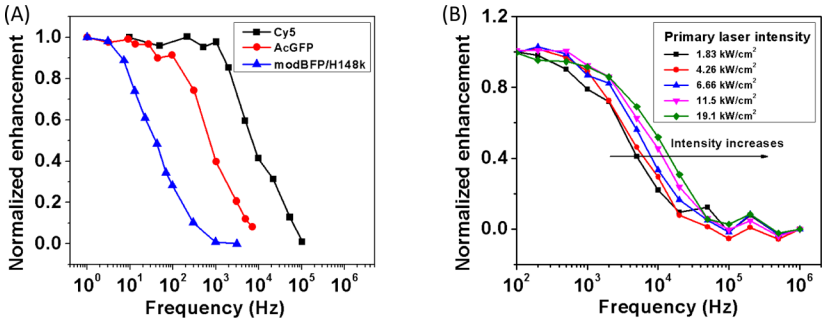

Figure 5. (A) Frequency response curves from Cy5, AcGFP, and modBFP/H148k in solution showing the span of the cutoff frequencies due to different photophysical on/off times. (B) Power-dependent cutoff frequency of Cy5 molecules in aqueous solution with constant 710 nm secondary excitation intensity (12 kW/cm^2) and varied 594 nm primary excitation intensity.

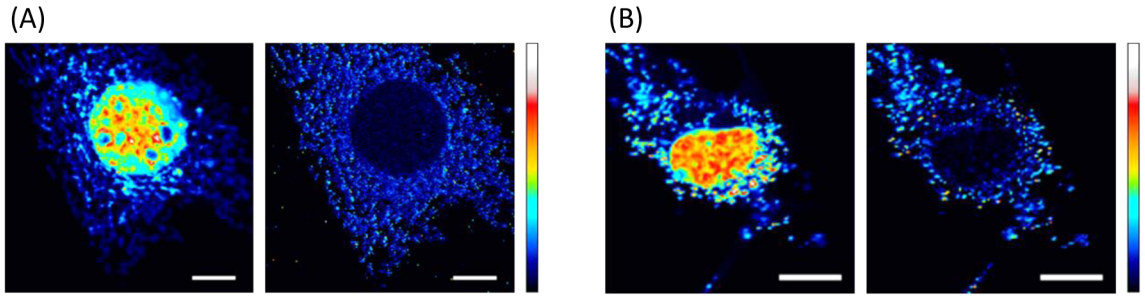

Figure 6. Selective fluorescence recovery of mitochondria-targeted AcGFP in the presence of high nuclear-targeted EGFP fluorescence for (A) fixed and (B) live NIH 3T3 cells: (leftmost images in (A) and (B)) raw fluorescence of AcGFP-labeled mitochondria and EGFP; (rightmost images in (A) and (B)) demodulated AcGFP fluorescence. SAFIRe efficiently eliminates the heterogeneous, unmodulatable EGFP signal and reveals a >10-fold improved contrast in the demodulated fluorescence images. For all of the images, the primary laser intensity was held at 5.9 kW/cm^2 and the secondary intensity (64 kW/cm^2) was modulated at 300 Hz. All scale bars are 10 μm. (Reproduced with permission from ref 9. Copyright 2012 American Chemical Society.)

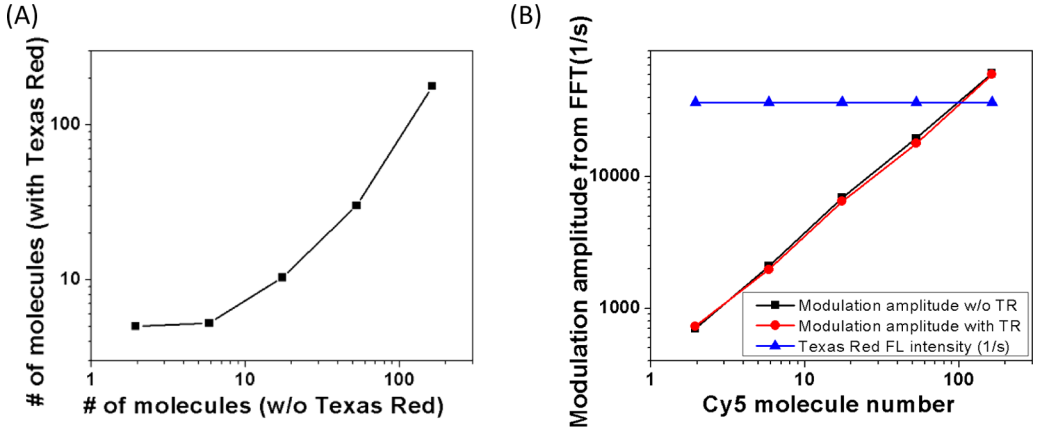

Figure 7. (A) Highly nonlinear titration of the numbers of Cy5 molecules with and without constant Texas Red background when FCS was used to determine the numbers of fluorophores. (B) Plots of FFT amplitude vs the number of Cy5 molecules, showing that the modulation amplitude is independent of the presence of the unmodulatable Texas Red background.

modulation frequency is directly encoded in the collected fluorescence, and therefore, SAFIRe does not need an exogenous reference signal for cross-correlation, but instead a lock-in amplifier or digital signal processing can be directly utilized without sacrificing signal (Figure 6). (3) SAFIRe is dynamic but has a characteristic frequency. This frequency results from the rates in and out of the dark state, enabling resolution of differently modulatable fluorophores based on dark-state lifetimes and the potential to directly probe the dynamics of complex systems. As only the fluorescence of interest is modulated, the waveform used to modulate the amplitude of the secondary laser serves as the reference for demodulation in either wide-field or confocal geometry (Figure 3C). The signal visibility gains coupled with the characteristic frequency response enable applications that both probe dynamics and visualize weak signals obscured by high, heterogeneous background (Figure 7).

7.1. Quantifying Fluorophore Concentrations in High-Background Solutions

To demonstrate the dynamic range of modulation for concentration determination, we diluted Cy5 at varying concentrations in (A) high Texas Red background and (B) pure, fluorescence-free water. Identical dilutions from the Cy5 stock solutions were used in the samples (A) and controls (B). Data were collected with dual laser excitation, exciting and

dx.doi.org/10.1021/ar400325y | Acc. Chem. Res. 2014, 47, 1545−1554

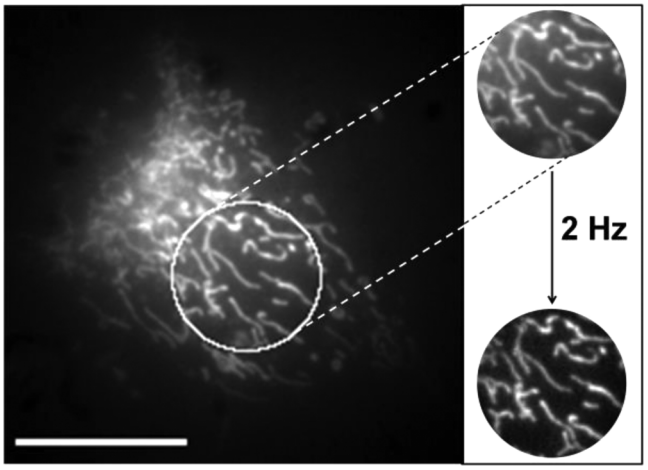

Figure 8. Live-cell demodulation of mitochondria-targeted modBFP/H148K. Upon 405 nm illumination, blue fluorescence was collected from modBFP/H148K-mito mixed with high background emission. Coillumination at 514.5 nm modulated at 2 Hz (secondary illumination only within the white circle) recovered only the modBFP/H148K-mito signal on a greatly reduced background (lower circle). The scale bar is 20 μm. (Reproduced with permission from ref 13. Copyright 2013 American Chemical Society.)

collecting the emission from both Cy5 and Texas Red. The secondary laser (710 nm) was amplitude-modulated at 1 kHz. Figure 7A shows the comparison between the apparent numbers of molecules with and without Texas Red background obtained by FCS. The curve is not linear because the high Texas Red background overwhelms the FCS analysis at low Cy5 copy numbers. In contrast, plotting the modulated signal amplitude (the amplitude at the modulation frequency in the Fourier domain) versus the number of Cy5 molecules as determined by FCS from the control yielded essentially identical linear curves for samples with and without Texas Red (Figure 7B). Thus, modulation recovered the true number of Cy5 molecules with linear scaling down to the single-molecule level independent of the fluorescent background.

7.2. Cellular Imaging and Fluorescent Protein Discrimination

Utilizing Ag nanodots,[8] organic dyes,[12] and fluorescent proteins,[9,13] we have employed SAFIRe to improve the contrast in fixed- and live-cell imaging. Figure 6 demonstrates that modulatable AcGFP-labeled features can be selectively recovered from both autofluorescence and spectrally indistinguishable but unmodulatble EGFP background in a modulated confocal geometry. The signal visibility was improved by >10-fold through SAFIRe-based demodulation with a lock-in amplifier. Analogously, although BFPs are typically rarely used because of problems with high autofluorescence background, we identified modulatable variants that enable wide-field SAFIRe imaging to essentially remove all of the autofluorescence background. We demonstrated signal gains of our SAFIRe scheme on mitochondria-targeted modBFP/H148K in live NIH 3T3 cells (Figure 8). The contrast for features of interest was again enhanced more than 5-fold after removal of the intrinsic inhomogeneous autofluorescence.

7.3. Selective Fluorescent Detection within Tissue Mimics

Medical imaging using fluorescence faces many substantial challenges. Penetration depths are typically sub-millimeter, even for near-IR wavelengths, and tissue autofluorescence poses detection challenges for low-concentration dyes buried at depths beyond 1 mm. To gauge the potential of SAFIRe-based detection for in vivo fluorescence studies, we embedded tissue-mimicking phantoms containing 100 nM (modulatable) Cy5 and 235 nM (unmodulatable) Texas Red within much larger non-Cy5-containing skin tissue mimics that were otherwise identical. All of the phantoms were composed of talc-France perfume powder (40 mg/mL), polystyrene beads (3 μm diameter, 1 mg/mL), and Texas Red (235 nM) in sodium alginate aqueous gels that were

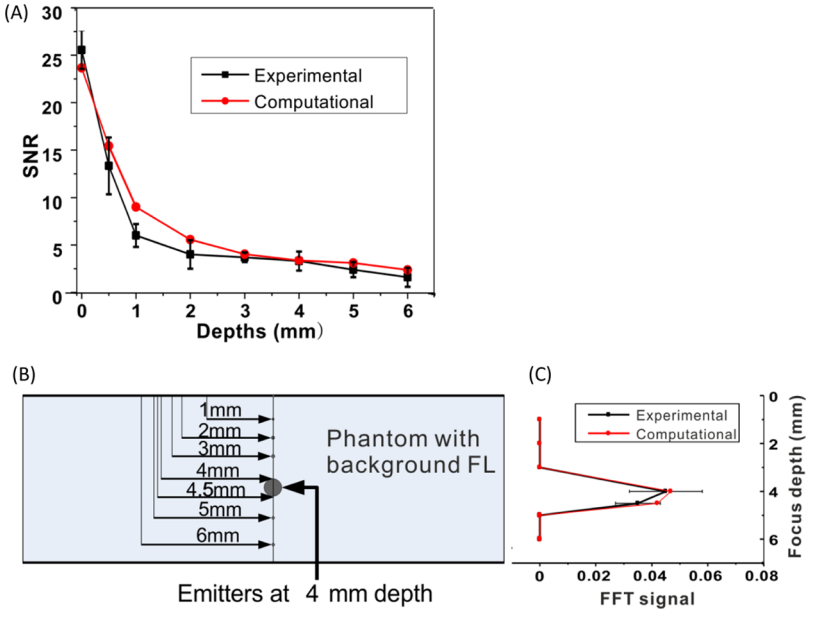

Figure 9. (A) Comparison of experimental and computed emission signals of Cy5 buried within high-background skin-tissue-mimicking phantoms. (B) Schematic of an emitter 4 mm deep within the tissue phantom. (C) Experimentally determined and finite element-calculated FFT signals at the 100 Hz modulation frequency when the 0.5 mm thick Cy5-loaded phantom was fixed at a depth of 4 mm. (Reproduced with permission from ref 10. Copyright 2013 American Chemical Society.)

dx.doi.org/10.1021/ar400325y | *Acc. Chem. Res.* 2014, 47, 1545−1554

cross-linked in 80 mM calcium chloride aqueous solution for 40 min. Texas Red was used to mimic intrinsic autofluorescence in real tissue.[10] As shown in Figure 9A, acceptable SNRs were obtained when the doped phantom was buried as deep as 6 mm within the highly scattering and brightly fluorescent skin tissue mimics. Furthermore, Figure 9B,C shows that we can correctly determine the depth of the Cy5-doped phantom. Because we modulate ground-state populations, many absorption-based contrast mechanisms become possible with analogous methods, all with laser intensities that should not exceed the maximum permissible skin exposure.

8. CONCLUSION

We have applied the principles of molecular modulation to fluorescence detection and live-cell imaging. By designing and characterizing new fluorophores for biological imaging, we have expanded the dimensionality of fluorescence imaging by using dark-state lifetime as an additional discriminating feature. Furthermore, the dark-state dynamics can now be studied in bulk, as characteristic lifetimes become observable without having to resort to single-molecule or fluctuation-based experiments. Because the dynamics change as a result of new time scales being present, a wide array of new experiments become possible to probe diffusion, binding, and photophysical dynamics in bulk studies that were previously unobservable. The long-wavelength modulation increases the fluorescence without generating any additional background in the higher-energy fluorescence detection channel. The fluorescence signal of interest is shifted away from all of the background to unique detection frequencies that have orders of magnitude lower noise, thereby enhancing both the signal visibility and sensitivity in complex, high-background systems. Signal visibilities in biological systems have been enhanced by up to 2 orders of magnitude, but further gains are possible as nearly shot-noise-limited detection is recovered. Through continued fluorophore development and utilization, we expect to make further sensitivity gains that enable ever finer features and dynamics to be probed in living systems.

AUTHOR INFORMATION

Corresponding Author

*E-mail: dickson@chemistry.gatech.edu.

Notes

The authors declare no competing financial interest.

Biographies

Jung-Cheng Hsiang received his M.S. in Physics in 2005 from National Taiwan University and subsequently enrolled as a Ph.D. student in the School of Physics at The Georgia Institute of Technology. Since he joined Dr. Robert Dickson's lab in 2006, his research has focused on single-molecule spectroscopy, primarily in understanding the photophysics and applications of silver nanoclusters. His efforts have largely defined the simulation and analysis methods that enable improved sensitivity and dynamic detection schemes afforded by modulation-based fluorescence signal recovery. Currently, his interests focus on molecular fluorescence simulations, analysis, and applications of SAFIRe for elucidating fast dynamics with subdiffraction resolution.

Amy E. Jablonski received her B.S. degree in Chemistry from the University of Alabama at Birmingham in 2007. As a Ph.D. student in the School of Chemistry and a member of Dr. Dickson's group, her research interests include the development and study of optical modulation of fluorescent proteins.

Robert Dickson earned degrees from Haverford College and The University of Chicago. After postdoctoral work at UCSD, he joined Georgia Tech's faculty in 1998, where he has pioneered the development and use of silver cluster and modulatable organic fluorophores to selectively recover weak signals buried within high background. With an eye toward medical imaging, current efforts in his lab involve the development of chromophores and tailored application of modulation-based signal recovery to spy on biologically relevant processes in their native environments.

ACKNOWLEDGMENTS

The authors gratefully acknowledge insight and assistance from our collaborators, C. J. Fahrni, A. Bommarius, and L. M. Tolbert, as well as the members of their groups. We also appreciate contributions from C. I. Richards, Y.-C. Chen, Chaoyang Fan, J. T. Petty, and S. Sarkar. This work was supported by NSF 0853692, NIH R01-GM086195, and NIH R56-AI107116.

REFERENCES

(1) Carpenter, J. F.; Crowe, J. H. An Infrared Spectroscopic Study of the Interactions of Carbohydrates with Dried Proteins. *Biochemistry* **1989**, *28*, 3916−3922.
(2) Moerner, W. E.; Kador, L. Optical detection and spectroscopy of single molecules in a solid. *Phys. Rev. Lett.* **1989**, *62*, 2535−2538.
(3) Min, W.; Lu, S.; Chong, S.; Roy, R.; Holtom, G. R.; Xie, X. S. Imaging chromophores with undetectable fluorescence by stimulated emission microscopy. *Nature* **2009**, *461*, 1105−1109.
(4) Schwille, P.; Haupts, U.; Maiti, S.; Webb, W. Molecular dynamics in living cells observed by fluorescence correlation spectroscopy with one- and two-photon excitation. *Biophys. J.* **1999**, *77*, 2251−2265.
(5) Patel, S. A.; Cozzuol, M.; Hales, J. M.; Richards, C. I.; Sartin, M.; Hsiang, J.-C.; Vosch, T.; Perry, J. W.; Dickson, R. M. Electron Transfer-Induced Blinking in Ag Nanodot Fluorescence. *J. Phys. Chem. C* **2009**, *113*, 20264−20270.
(6) Resch-Genger, U.; Grabolle, M.; Cavaliere-Jaricot, S.; Nitschke, R.; Nann, T. Quantum dots versus organic dyes as fluorescent labels. *Nat. Methods* **2008**, *5*, 763−775.
(7) Shaner, N. C.; Steinbach, P. A.; Tsien, R. Y. A guide to choosing fluorescent proteins. *Nat. Methods* **2005**, *2*, 905−909.
(8) Richards, C. I.; Hsiang, J.-C.; Senapati, D.; Patel, S.; Yu, J. H.; Vosch, T.; Dickson, R. M. Optically Modulated Fluorophores for Selective Fluorescence Signal Recovery. *J. Am. Chem. Soc.* **2009**, *131*, 4619−4621.
(9) Jablonski, A.; Hsiang, J.-C.; Bagchi, P.; Hull, N.; Richards, C. I.; Fahrni, C. J.; Dickson, R. M. Signal Discrimination Between Fluorescent Proteins in Live Cells by Long-Wavelength Optical Modulation. *J. Phys. Chem. Lett.* **2012**, *3*, 3585−3591.
(10) Sarkar, S.; Fan, C.; Hsiang, J.-C.; Dickson, R. M. Modulated Fluorophore Signal Recovery Buried within Tissue Mimicking Phantoms. *J. Phys. Chem. A* **2013**, *117*, 9501−9509.
(11) Fan, C. Y.; Hsiang, J.-C.; Dickson, R. M. Optical Modulation and Selective Recovery of Cy5 Fluorescence. *ChemPhysChem* **2012**, *13*, 1023−1029.
(12) Fan, C. Y.; Hsiang, J.-C.; Jablonski, A. E.; Dickson, R. M. All-optical fluorescence image recovery using modulated stimulated emission depletion. *Chem. Sci.* **2011**, *2*, 1080−1085.
(13) Jablonski, A. E.; Vegh, R. B.; Hsiang, J.-C.; Bommarius, B.; Chen, Y.-C.; Solntsev, K. M.; Bommarius, A. S.; Tolbert, L. M.; Dickson, R. M. Optically modulatable blue fluorescent proteins. *J. Am. Chem. Soc.* **2013**, *135*, 16410−16417.
(14) Richards, C. I.; Hsiang, J.-C.; Dickson, R. M. Synchronously Amplified Fluorescence Image Recovery (SAFIRe). *J. Phys. Chem. B* **2010**, *114*, 660−665.
(15) Richards, C. I.; Hsiang, J.-C.; Khalil, A. M.; Hull, N. P.; Dickson, R. M. FRET-Enabled Optical Modulation for High Sensitivity Fluorescence Imaging. *J. Am. Chem. Soc.* **2010**, *132*, 6318−6323.

(16) Dahan, M.; Laurence, T.; Pinaud, F.; Chemla, D. S.; Alivisatos, A. P.; Sauer, M.; Weiss, S. Time-gated biological imaging by use of colloidal quantum dots. *Opt. Lett.* **2001**, *26*, 825−827.
(17) Marriott, G.; Mao, S.; Sakata, T.; Ran, J.; Jackson, D. K.; Petchprayoon, C.; Gomez, T. J.; Warp, E.; Tulyathan, O.; Aaron, H. L.; Isacoff, E. Y.; Yan, Y. L. Optical lock-in detection imaging microscopy for contrast-enhanced imaging in living cells. *Proc. Natl. Acad. Sci. U.S.A.* **2008**, *105*, 17789−17794.
(18) Tian, Z. Y.; Li, A. D. Q. Photoswitching-Enabled Novel Optical Imaging: Innovative Solutions for Real-World Challenges in Fluorescence Detections. *Acc. Chem. Res.* **2013**, *46*, 269−279.
(19) Ringemann, C.; Schoenle, A.; Giske, A.; Von Middendorff, C.; Hell, S. W.; Eggeling, C. Enhancing fluorescence brightness: Effect of reverse intersystem crossing studied by fluorescence fluctuation spectroscopy. *ChemPhysChem* **2008**, *9*, 612−624.
(20) Petty, J. T.; Story, S. P.; Hsiang, J.-C.; Dickson, R. M. DNA-Templated Molecular Silver Fluorophores. *J. Phys. Chem. Lett.* **2013**, *4*, 1148−1155.
(21) Petty, J. T.; Zheng, J.; Hud, N. V.; Dickson, R. M. DNA-Templated Ag Nanocluster Formation. *J. Am. Chem. Soc.* **2004**, *126*, 5207−5212.
(22) Choi, S.; Dickson, R. M.; Yu, J. H. Developing luminescent silver nanodots for biological applications. *Chem. Soc. Rev.* **2012**, *41*, 1867−1891.
(23) Richards, C. I.; Choi, S.; Hsiang, J.-C.; Antoku, Y.; Vosch, T.; Bongiorno, A.; Tzeng, Y.-L.; Dickson, R. M. Oligonucleotide-stabilized Ag nanocluster fluorophores. *J. Am. Chem. Soc.* **2008**, *130*, 5038−5039.
(24) Vosch, T.; Antoku, Y.; Hsiang, J.-C.; Richards, C. I.; Gonzalez, J. I.; Dickson, R. M. Strongly emissive individual DNA-encapsulated Ag nanoclusters as single-molecule fluorophores. *Proc. Natl. Acad. Sci. U.S.A.* **2007**, *104*, 12616−12621.
(25) Henglein, A.; Mulvaney, P.; Linnert, T. Chemistry of Ag_n Aggregates in Aqueous Solution: Non-metallic Oligomeric Clusters and Metallic Particles. *Faraday Discuss.* **1991**, *92*, 31−44.
(26) Gratz, H.; Penzkofer, A. Saturable absorption dynamics in the triplet system and triplet excitation induced singlet fluorescence of some organic molecules. *Chem. Phys.* **2001**, *263*, 471−490.
(27) Huang, Z. X.; Ji, D. M.; Wang, S. F.; Xia, A. D.; Koberling, F.; Patting, M.; Erdmann, R. Spectral identification of specific photophysics of Cy5 by means of ensemble and single molecule measurements. *J. Phys. Chem. A* **2006**, *110*, 45−50.
(28) Tinnefeld, P.; Buschmann, V.; Weston, K. D.; Sauer, M. Direct observation of collective blinking and energy transfer in a bichromophoric system. *J. Phys. Chem. A* **2003**, *107*, 323−327.
(29) Eggeling, C.; Widengren, J.; Brand, L.; Schaffer, J.; Felekyan, S.; Seidel, C. A. M. Analysis of photobleaching in single-molecule multicolor excitation and Förster resonance energy transfer measurements. *J. Phys. Chem. A* **2006**, *110*, 2979−2995.
(30) Jares-Erijman, E. A.; Jovin, T. M. FRET imaging. *Nat. Biotechnol.* **2003**, *21*, 1387−1395.
(31) Hanninen, P. E.; Lehtela, L.; Hell, S. W. Two- and multiphoton excitation of conjugate-dyes using a continuous wave laser. *Opt. Commun.* **1996**, *130*, 29−33.
(32) Schonle, A.; Hanninen, P. E.; Hell, S. W. Nonlinear fluorescence through intermolecular energy transfer and resolution increase in fluorescence microscopy. *Ann. Phys (Berlin)* **1999**, *8*, 115−133.
(33) Zhou, X. X.; Lin, M. Z. Photoswitchable fluorescent proteins: Ten years of colorful chemistry and exciting applications. *Curr. Opin. Chem. Biol.* **2013**, *17*, 682−690.
(34) Dickson, R. M.; Cubitt, A. B.; Tsien, R. Y.; Moerner, W. E. On/off blinking and switching behaviour of single molecules of green fluorescent protein. *Nature* **1997**, *388*, 355−358.
(35) Yokoe, E.; Meyer, T. Spatial dynamics of GFP-tagged proteins investigated by local fluorescence enhancement. *Nat. Biotechnol.* **1996**, *14*, 1252−1256.
(36) Ando, R.; Mizuno, H.; Miyawaki, A. Regulated fast nucleocytoplasmic shuttling observed by reversible protein highlighting. *Science* **2004**, *306*, 1370−1373.
(37) Sinnecker, D.; Voigt, P.; Hellwig, N.; Schaefer, M. Reversible photobleaching of enhanced green fluorescent proteins. *Biochemistry* **2005**, *44*, 7085−7094.
(38) Leiderman, P.; Genosar, L.; Huppert, D.; Shu, X.; Remington, S. J.; Solntsev, K. M.; Tolbert, L. M. Ultrafast Excited-State Dynamics in the Green Fluorescent Protein Variant S65T/H148D. 3. Short- and Long-Time Dynamics of the Excited-State Proton Transfer. *Biochemistry* **2007**, *46*, 12026−12036.
(39) Lakowicz, J. R. *Principles of Fluorescence Spectroscopy*, 3rd ed.; Springer: New York, 2006.